

# Purinergic P2X<sub>7</sub> Receptors Mediate ATP-induced Saliva Secretion by the Mouse Submandibular Gland\*

Received for publication, November 12, 2008. Published, JBC Papers in Press, December 19, 2008, DOI 10.1074/jbc.M808597200

Tetsuji Nakamoto<sup>‡§1,2</sup>, David A. Brown<sup>‡1</sup>, Marcelo A. Catalán<sup>‡1</sup>, Mireya Gonzalez-Begne<sup>‡</sup>, Victor G. Romanenko<sup>‡§</sup>, and James E. Melvin<sup>‡§3</sup>

From the <sup>‡</sup>Center for Oral Biology and the <sup>§</sup>Department of Pharmacology & Physiology, University of Rochester Medical Center, Rochester, New York 14642

Salivary glands express multiple isoforms of P2X and P2Y nucleotide receptors, but their *in vivo* physiological roles are unclear. P2 receptor agonists induced salivation in an *ex vivo* submandibular gland preparation. The nucleotide selectivity sequence of the secretion response was BzATP  $\gg$  ATP  $>$  ADP  $\gg$  UTP, and removal of external Ca<sup>2+</sup> dramatically suppressed the initial ATP-induced fluid secretion (~85%). Together, these results suggested that P2X receptors are the major purinergic receptor subfamily involved in the fluid secretion process. Mice with targeted disruption of the P2X<sub>7</sub> gene were used to evaluate the role of the P2X<sub>7</sub> receptor in nucleotide-evoked fluid secretion. P2X<sub>7</sub> receptor protein and BzATP-activated inward cation currents were absent, and importantly, purinergic receptor agonist-stimulated salivation was suppressed by more than 70% in submandibular glands from P2X<sub>7</sub>-null mice. Consistent with these observations, the ATP-induced increases in [Ca<sup>2+</sup>]<sub>i</sub> were nearly abolished in P2X<sub>7</sub><sup>-/-</sup> submandibular acinar and duct cells. ATP appeared to also act through the P2X<sub>7</sub> receptor to inhibit muscarinic-induced fluid secretion. These results demonstrate that the ATP-sensitive P2X<sub>7</sub> receptor regulates fluid secretion in the mouse submandibular gland.

Salivation is a Ca<sup>2+</sup>-dependent process (1, 2) primarily associated with the neurotransmitters norepinephrine and acetylcholine, release of which stimulates  $\alpha$ -adrenergic and muscarinic receptors, respectively. Both types of receptors are coupled to G proteins that activate phospholipase C $\beta$  (PLC $\beta$ ) during salivary gland stimulation. PLC $\beta$  activation cleaves phosphatidylinositol 1,4-bisphosphate resulting in diacylglycerol and inositol 1,4,5-trisphosphate (InsP<sub>3</sub>) production. Activation of Ca<sup>2+</sup>-selective InsP<sub>3</sub> receptor channels localized to the endoplasmic reticulum of salivary acinar cells increases the

intracellular free calcium concentration ([Ca<sup>2+</sup>]<sub>i</sub>).<sup>4</sup> Depletion of the endoplasmic reticulum Ca<sup>2+</sup> pool triggers extracellular Ca<sup>2+</sup> influx and a sustained elevation in [Ca<sup>2+</sup>]<sub>i</sub>. This increase in [Ca<sup>2+</sup>]<sub>i</sub> activates Ca<sup>2+</sup>-dependent K<sup>+</sup> and Cl<sup>-</sup> channels promoting Cl<sup>-</sup> secretion across the apical membrane and a lumen negative, electrochemical gradient that supports Na<sup>+</sup> efflux into the lumen. The accumulation of NaCl creates an osmotic gradient which drives water movement into the lumen, thus generating isotonic primary saliva. This primary fluid is then modified by the ductal system, which reabsorbs NaCl and secretes KHCO<sub>3</sub> producing a final saliva that is hypotonic (1, 2).

Salivation also has a non-cholinergic, non-adrenergic component, the origin of which is unclear (3). In addition to muscarinic and  $\alpha$ -adrenergic receptors, salivary acinar cells express other receptors that are coupled to an increase in [Ca<sup>2+</sup>]<sub>i</sub>, such as purinergic P2 and substance P receptors. Like muscarinic and  $\alpha$ -adrenergic receptors, P2 receptor activation leads to a sustained increase in [Ca<sup>2+</sup>]<sub>i</sub> in salivary acinar cells (4). In contrast, substance P receptor activation rapidly desensitizes and therefore generates only a relatively transient increase in [Ca<sup>2+</sup>]<sub>i</sub> (5) that is unlikely to appreciably contribute to fluid secretion. The purinergic P2 receptor family is comprised of G protein-coupled P2Y and ionotropic P2X receptors activated by extracellular di- and triphosphate nucleotides. Activation of both subfamilies of P2 receptors causes an increase in [Ca<sup>2+</sup>]<sub>i</sub>. P2Y receptors increase [Ca<sup>2+</sup>]<sub>i</sub> via InsP<sub>3</sub>-induced Ca<sup>2+</sup> mobilization from intracellular stores (similar to  $\alpha$ -adrenergic and muscarinic receptors) while P2X receptors act as ligand-gated, non-selective cation channels that mediate extracellular Ca<sup>2+</sup> influx (6). Salivary gland tissues express at least four isoforms of P2X (P2X<sub>4</sub> and P2X<sub>7</sub>) and P2Y (P2Y<sub>1</sub> and P2Y<sub>2</sub>) subtypes; however, their *in vivo* physiological significance has yet to be characterized (7–11).

Our results revealed that ATP acts in isolation to stimulate fluid secretion from the mouse submandibular gland, but secretion is inhibited when ATP is simultaneously presented with a muscarinic receptor agonist. Ablation of the P2X<sub>7</sub> gene had no effect on the salivary flow rate evoked by muscarinic receptor activation, but markedly reduced ATP-mediated fluid secretion and rescued the inhibitory effects of ATP on muscarinic receptor activation. Submandibular gland acinar cells from P2X<sub>7</sub><sup>-/-</sup>

\* This work was supported, in whole or in part, by National Institutes of Health Grants DE09692 and DE08921 (to J. E. M.) and NIDCR Training Grant T32-DE07202 (to D. A. B. and M. G.-B.). The costs of publication of this article were defrayed in part by the payment of page charges. This article must therefore be hereby marked "advertisement" in accordance with 18 U.S.C. Section 1734 solely to indicate this fact.

<sup>1</sup> These authors contributed equally to this work.

<sup>2</sup> Present address: Dept. of Oral Reconstruction and Rehabilitation, Kyushu Dental College, 2-6-1 Manazuru, Kokurakita-ku, Kitakyushu City 803-8580, Japan.

<sup>3</sup> To whom correspondence should be addressed: Center for Oral Biology, Box 611, University of Rochester Medical Center, 601 Elmwood Ave., Rochester, NY 14642. Tel.: 585-275-3441; Fax: 585-506-0190; E-mail: james\_melvin@urmc.rochester.edu.

<sup>4</sup> The abbreviations used are: [Ca<sup>2+</sup>]<sub>i</sub>, intracellular free calcium concentration; BzATP, 2',3'-O-(4-benzoylbenzoyl)adenosine 5'-triphosphate; SMG, submandibular gland(s); CCh, carbachol; GPCR, G protein-coupled receptors; SLG, sublingual; PG, parotid; ANOVA, analysis of variance; BSA, bovine serum albumin.

## ATP-stimulated Fluid Secretion

animals had dramatically impaired ATP-activated  $\text{Ca}^{2+}$  signaling, consistent with this being the mechanism responsible for the reduction in ATP-mediated fluid secretion in these mice. Together, these results demonstrated that ATP regulates salivation, acting mainly through the  $\text{P2X}_7$  receptor. Activation of the  $\text{P2X}_7$  receptor may play a major role in non-adrenergic, non-cholinergic stimulated fluid secretion.

### EXPERIMENTAL PROCEDURES

**General Methods**—Mice were housed in microisolator cages with *ad libitum* access to laboratory chow and water during 12-hour light/dark cycles. An equal number of gender- and age-matched (2–6-month-old) animals were utilized. Black Swiss/129 SvJ hybrid (Rochester colony) and C57BL/6 strain mice were obtained from Jackson Laboratories (Bar Harbor, ME), while  $\text{P2X}_7^{-/-}$  C57BL/6 mice were obtained from Pfizer (Benton, CT) and used as indicated. All experimental protocols were approved by the University of Rochester Animal Resources Committee. Reagents were obtained from Sigma unless otherwise specified.

**Ex Vivo Submandibular Gland (SMG) Perfusion**—*Ex vivo* SMG perfusion was performed as previously reported (12, 13). In brief, mice were anesthetized with an intraperitoneal injection of chloral hydrate (400 mg/kg body weight). Following ligation of all branches of the common carotid artery except the SMG artery, the SMG was removed, cannulated, and perfused. The *ex vivo* perfusion solution contained (in mM): 4.3 KCl, 120 NaCl, 25  $\text{NaHCO}_3$ , 5 glucose, 10 HEPES, 1  $\text{CaCl}_2$ , 1  $\text{MgCl}_2$ , pH 7.4. Extracellular  $\text{Ca}^{2+}$ -free solutions were made by removing  $\text{CaCl}_2$ . Solutions maintained at 37 °C were gassed with 95%  $\text{O}_2$ , 5%  $\text{CO}_2$ , and perfused at 0.8 ml/min using a peristaltic pump. When stimulating with only purinergic receptor agonists, muscarinic and  $\beta$ -adrenergic receptor antagonists were included (0.5  $\mu\text{M}$  atropine and 20  $\mu\text{M}$  propranolol, respectively).

Once the gland began to secrete fluid (defined as time 0), stimulation was continued for an additional 10 min. Saliva was collected in pre-calibrated capillary tubes (Sigma-Aldrich), and volumes were recorded every 0.5 or 1 min to calculate the flow rate ( $\mu\text{l}/\text{min}$ ). Following saliva collection, the gland was blot dried and weighed. Saliva samples were stored at –86 °C until further analysis.  $\text{Na}^+$  and  $\text{K}^+$  concentrations were analyzed by atomic absorption using a Perkin-Elmer 3030 spectrophotometer. The  $\text{Cl}^-$  concentration was analyzed with an Expandable Ion Analyzer EA 940 (Orion Research), and the pH and the osmolality were measured with a pH-sensitive electrode (Thermo Scientific, Beverly, MA) and a Wescor 5500 Vapor Pressure Osmometer (Logan, Utah), respectively.

**In Vitro  $[\text{Ca}^{2+}]_i$  Measurement**—SMG ductal and acinar cells were prepared by enzyme digestion as previously reported (14). In brief, mice were euthanized by 100%  $\text{CO}_2$  exposure followed by cardiac puncture. Acinar cells were dispersed in Minimum Essential Medium (SMEM, Invitrogen) supplemented with 1% bovine serum albumin (BSA), 0.17 mg/ml Liberase-RI (Roche Applied Science), and 2 mM L-glutamine, whereas duct cells were dispersed in Minimum Essential Medium (SMEM, Invitrogen) supplemented with 1% BSA, 0.012% trypsin, 0.05 mM EDTA, and 2 mM L-glutamine. Trypsin digestion was stopped with 2 mg/ml of soybean trypsin inhibitor. Duct cells

were further dispersed by additional digestion in Minimum Essential Medium (SMEM) supplemented with 1% BSA, 0.15 units/ml Liberase-RI, and 2 mM L-glutamine. Following digestion, acinar and duct cells were rinsed in Basal Medium Eagle (BME, Invitrogen) supplemented with 1% BSA.

The fluorescent dye Fura-2 was used for  $[\text{Ca}^{2+}]_i$  measurement. Cells were loaded by incubation with 2  $\mu\text{M}$  Fura-2 AM (Invitrogen) for 20 min at room temperature. Imaging was performed using an inverted microscope (Nikon Diaphot 200) equipped with an imaging system (Till Photonics, Pleasanton, CA). Images from Fura-2-loaded cells were acquired at a rate of 1 Hz by alternate excitation of light at 340 nm and 380 nm, and emission was captured at 510 nm using a high speed digital camera (Till Photonics). Chamber volume was maintained at ~400  $\mu\text{l}$ . Cells were superfused at a rate of 4 ml/min with the *ex vivo* perfusion solution (37 °C). The fluorescence ratio of 340 nm over 380 nm was calculated, and all data are presented as the change in ratio units.

**Enrichment of Biotinylated Plasma Membrane Proteins**—Isolated SMG acinar cells (14) were biotinylated according to the manufacturer's instructions (Pierce), and the plasma membrane proteins enriched as previously described (15). In brief, biotinylated cells were collected by centrifugation at 1,000  $\times g$  for 45 s, and the pellet homogenized twice in ice-cold homogenizing buffer containing: 250 mM sucrose, 10 mM triethanolamine, 1  $\mu\text{g}/\text{ml}$  leupeptin, and 0.1 mg/ml phenylmethanesulfonyl fluoride. Unbroken cells and nuclei were pelleted at 4,000  $\times g$  for 10 min at 4 °C and discarded. The supernatants were centrifuged at 22,000  $\times g$  for 20 min at 4 °C. The resulting pellet was resuspended in homogenization buffer, centrifuged at 46,000  $\times g$  (Beckman SW28 rotor) for 30 min at 4 °C, and the crude pellet was resuspended in 1 ml of hypotonic buffer (100 mM  $\text{NH}_4\text{HCO}_3$ , pH 7.5, 5 mM  $\text{MgCl}_2$ ) followed by incubation overnight with 200  $\mu\text{l}$  of Dynabeads M-280 streptavidin (Invitrogen Dynal AS; Carlsbad, CA) at 4 °C. Beads were collected with a magnetic plate and washed with hypotonic buffer. Streptavidin beads carrying the enriched plasma membrane fractions were suspended in 100 mM dithiothreitol for 2 h, centrifuged at 10,600  $\times g$  for 3 min, and the supernatants collected and used for immunoblotting.

**Electrophoresis and Immunoblot Analysis**—Protein samples (30  $\mu\text{g}$ ) were boiled for 5 min prior to separation in a 10% SDS-PAGE Tris-glycine mini-gel (Bio-Rad). Protein was transferred overnight at 4 °C onto polyvinylidene difluoride membranes (Invitrogen) as described previously (15). Membranes were blocked overnight at 4 °C with 5% nonfat dry milk in 25 mM Tris pH 7.5, 150 mM NaCl (TBS) and then incubated at 4 °C overnight with primary antibody raised against the 576–595 C terminus of the rat  $\text{P2X}_7$  receptor (Millipore-Chemicon International Inc., Temecula, CA) at a dilution of 1:300 in a 2.5% nonfat dry milk solution. After washing with TBS containing 0.05% Tween-20 (TBS-T), the membranes were incubated with horseradish peroxidase-conjugated goat anti-rabbit IgG secondary antibody (Pierce) at a dilution of 1:2,500 in TBS-T/2.5% nonfat dry milk for 1 h at room temperature. Proteins were visualized using enhanced chemiluminescence (GE-Amersham Biosciences, Piscataway, NJ).

**Electrophysiological Recordings**—Single SMG acinar cells were prepared by enzymatic digestion (13). In brief, SMG acinar cells were digested for 15 min in SMEM containing 0.02% trypsin (Invitrogen), then centrifuged and resuspended in medium containing soybean trypsin inhibitor (Type 1-S, Sigma), followed by 2 sequential digestions for 25 min each in 0.17 mg/ml Liberase RI Enzyme (Roche Applied Science, Indianapolis, IN). The cell suspension was gently centrifuged and the supernatant filtrated through a 53- $\mu$ m nylon mesh. Finally, the suspension was centrifuged, and the cell pellet was resuspended in BME supplemented with 2 mM L-glutamine (Invitrogen). Cells were maintained at 37 °C in a 5% CO<sub>2</sub> humidified incubator until use.

Electrophysiological data were acquired at room temperature using a PC-501A amplifier (Warner Instrument, Hamden, CT) or an Axopatch 200B amplifier (Molecular Devices, Sunnyvale, CA). Voltage pulses were generated with Clampex 9 software through a Digidata 1320A interface (Molecular Devices), which also served to acquire the currents. Voltage clamp experiments were performed using the standard whole-cell configuration of the patch clamp technique. Glass pipettes (Warner Instrument) were pulled to give a resistance of 2–3 M $\Omega$  in the solutions described below. The external solution contained (in mM): 150 NaCl, 1 CaCl<sub>2</sub>, 1 MgCl<sub>2</sub>, 10 HEPES, 20 sucrose, pH 7.4. The internal pipette solution contained (in mM): 130 Cs glutamate (130 CsOH + 130 glutamic acid), 10 NaCl, 1 MgCl<sub>2</sub>, 1.5 EGTA, 10 HEPES, pH 7.3. Single mouse SMG acinar cells were voltage clamped at E<sub>Cl</sub> (–63.8 mV). Liquid junction potential was calculated to be 17.3 mV, and the correction was applied to the voltage.

**Statistical Analysis**—Results are presented as the mean  $\pm$  S.E. Statistical significance was determined using Student's *t* test or ANOVA analysis, followed by a Bonferroni's test for multiple comparisons with Origin 7.0 Software (OriginLab, Northampton, MA). *p* values of less than 0.05 were considered statistically significant. All experiments were performed using three or more separate preparations.

## RESULTS

**Purinergic Receptor Agonists Evoke Fluid Secretion from the *ex Vivo* SMG**—Salivary glands express several types of purinergic receptors which belong to both the P2X (P2X<sub>4</sub> and P2X<sub>7</sub>) and P2Y (P2Y<sub>1</sub> and P2Y<sub>2</sub>) receptor subfamilies (10, 11). Given that activation of P2X and P2Y receptors evokes an increase in [Ca<sup>2+</sup>]<sub>i</sub> in salivary gland cells, purinergic stimulation of either subfamily might be expected to result in fluid secretion (2). However, purinergic receptor activation has not been previously performed in the intact gland. To test this hypothesis we employed an *ex vivo*, perfused mouse SMG organ system. This *ex vivo* technique allows for precise control of the content of the vascular perfusate and ameliorates the rapid degradation of purinergic receptor agonists observed *in vivo*.

Most G protein-coupled P2Y receptors are sensitive to UTP whereas the ionotropic P2X receptors are not, while both classes of P2 receptors are generally activated by ATP and ADP (6). To determine if purinergic receptor activation produced saliva secretion in the *ex vivo* SMG preparation we initially utilized the ubiquitous P2 receptor activator ATP. Fig. 1A shows

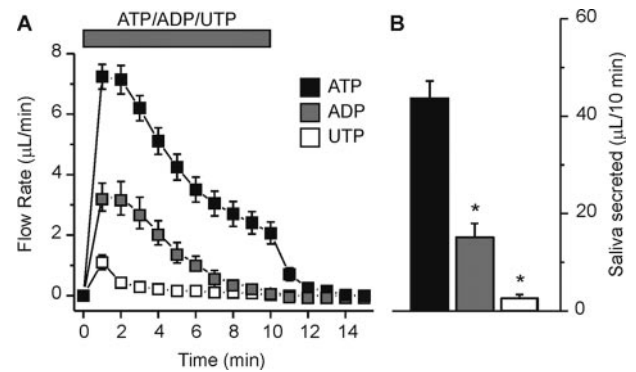


**FIGURE 1. Purinergic P2 receptor agonists evoked fluid secretion in the *ex vivo* SMG.** Agonists (1 mM) were applied to the *ex vivo*, perfused SMG for 10 min as indicated by the bar. *A*, flow rate following stimulation with ATP (black squares), ADP (gray squares), or UTP (white squares). *B*, summary of the results shown in panel *A* as the total volume of fluid secreted over the 10-min stimulation period. Data were from an equal number of male and female animals for ATP, ADP, and UTP ( $n = 12$ ,  $n = 10$ , and  $n = 10$  glands, respectively; \*,  $p < 0.001$ ). Black Swiss/129 SvJ mice were used for these experiments.

that the time course of the secretion generated by stimulation of the *ex vivo* SMG by ATP (1 mM) was best described as having an initial peak during the first 2 min followed over the next 8 min by a gradual decline to a relatively sustained fluid secretion rate (Fig. 1A, black squares). A relatively rapid loss of secretion was observed after the removal of ATP from the perfusate. To further characterize which P2 receptor was likely involved we also tested the ability of ADP and UTP to stimulate secretion. ADP (1 mM) produced a similar pattern as observed during ATP stimulation (Fig. 1A, gray squares), but the total amount of saliva produced during a 10-min stimulation was significantly less (Fig. 1B, ADP;  $15.2 \pm 2.8 \mu\text{L}/10 \text{ min}$  versus ATP;  $43.7 \pm 3.5 \mu\text{L}/10 \text{ min}$ ,  $p < 0.001$ ). Stimulation with UTP (1 mM) produced a transient flow (Fig. 1A, white squares) which generated markedly less fluid, ~6% of the saliva secreted with an identical concentration of ATP (Fig. 1B, UTP;  $2.7 \pm 0.7 \mu\text{L}/10 \text{ min}$  versus ATP;  $43.7 \pm 3.5 \mu\text{L}/10 \text{ min}$ ,  $p < 0.001$ ).

**Extracellular Ca<sup>2+</sup> Depletion Suppresses ATP-induced Salivation by the *ex Vivo* SMG**—UTP does not activate P2X receptors (6). Accordingly, because UTP caused minimal fluid secretion (Fig. 1), it appeared that P2Y receptors do not play a major role in the purinergic-induced production of saliva. Therefore, we next evaluated the role of P2X receptors in ATP-mediated, Ca<sup>2+</sup>-dependent fluid secretion. Although both couple to an increase in [Ca<sup>2+</sup>]<sub>i</sub>, one fundamental difference between P2Y and P2X receptors is that P2X receptors mediate extracellular Ca<sup>2+</sup> entry, whereas P2Y receptors initially trigger intracellular Ca<sup>2+</sup> release. Consequently, acute removal of extracellular Ca<sup>2+</sup> effectively eliminates Ca<sup>2+</sup> influx via P2X channels, but the intracellular Ca<sup>2+</sup> release mediated by P2Y receptors is resistant to this maneuver.

Using the muscarinic agonist carbachol (CCh), which activates an identical Ca<sup>2+</sup> release GPCR pathway as P2Y receptors, we show that initial secretion by the *ex vivo* SMG was not significantly affected by acute removal of extracellular Ca<sup>2+</sup>. CCh-evoked (0.3  $\mu\text{M}$ ) SMG fluid secretion in the absence of extracellular Ca<sup>2+</sup> (black squares) was similar to secretion in Ca<sup>2+</sup>-containing experiments (gray squares) during the first

## ATP-stimulated Fluid Secretion

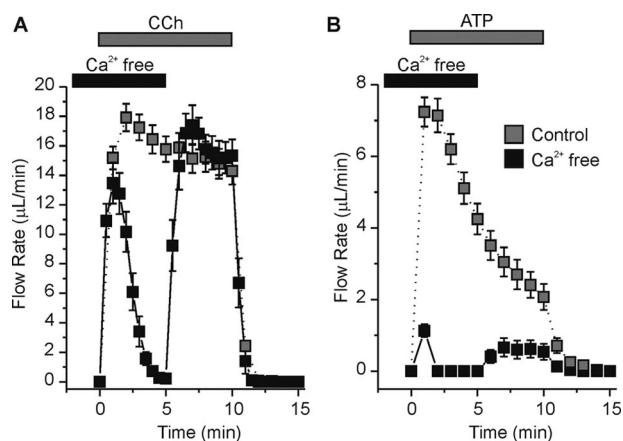


**FIGURE 2. Extracellular  $\text{Ca}^{2+}$  removal abolished ATP-induced fluid secretion in the *ex vivo* SMG.** Agonists were applied to the *ex vivo*, perfused SMG for 10 min as indicated by the gray bar. For  $\text{Ca}^{2+}$ -free experiments (black squares), glands were perfused with extracellular  $\text{Ca}^{2+}$ -free solution for 2 min prior to stimulation and extracellular  $\text{Ca}^{2+}$  was re-introduced to the perfusate following 5 min of stimulation as indicated by the black bar. **A**,  $0.3 \mu\text{M}$  CCh-evoked fluid secretion in the presence (gray squares) or absence (black squares) of extracellular  $\text{Ca}^{2+}$ . **B**,  $1 \text{ mM}$  ATP-evoked fluid secretion in the presence (gray squares) or absence (black squares) of extracellular  $\text{Ca}^{2+}$ . CCh- and ATP-evoked fluid secretions were from an equal number of male and female animals ( $n = 8$  glands for each condition). Black Swiss/129 SvJ mice were used for these experiments.

minute of stimulation (Fig. 2A). However, without extracellular  $\text{Ca}^{2+}$  influx to replenish the rapidly depleted intracellular  $\text{Ca}^{2+}$  stores, the flow rate was eventually reduced to near zero (Fig. 2A, black trace at 4-min stimulation). Replacing extracellular  $\text{Ca}^{2+}$  after 5 min of CCh stimulation restored the flow rate to control values (Fig. 2A, black trace at 6–10 min stimulation). Secretion rapidly returned to basal levels upon removal of CCh from the perfusate. Using the same paradigm, the ATP-evoked ( $1 \text{ mM}$ ) fluid secretion was nearly abolished except for a very small volume secreted during the first minute of stimulation (Fig. 2B, black trace; ~85% decrease). Re-addition of extracellular  $\text{Ca}^{2+}$  resulted in a modest recovery of the fluid secretion flow rate (Fig. 2B, black versus gray trace at 6–10-min stimulation). Because UTP stimulated little secretion and because the initial ATP-mediated saliva secretion was dependent upon extracellular  $\text{Ca}^{2+}$ , our results suggested that ATP activated a member of the P2X family of channels. To determine which P2X isoform was involved, both pharmacological and genetic approaches were utilized in the following experiments.

**The  $\text{P2X}_7$  Receptor-selective Activator BzATP Stimulates Fluid Secretion**—Salivary glands have been shown to express both  $\text{P2X}_4$  and  $\text{P2X}_7$  receptors (10). To differentiate between potential activation of  $\text{P2X}_4$  or  $\text{P2X}_7$  receptors in our *ex vivo* SMG fluid secretion experiments we utilized the ATP-derivative BzATP.  $\text{P2X}_7$  receptors are activated preferentially by BzATP over ATP (16); thus, BzATP has served as a classical tool to evaluate  $\text{P2X}_7$  receptor function. Concentrations of ATP and BzATP were selected to avoid maximum flow rates. Fluid secretion was often detectable at agonist concentrations as low as  $0.1 \text{ mM}$  for ATP (data not shown); however, fluid secretion was always observed at agonist concentrations of  $0.25 \text{ mM}$  and higher. Fig. 3 shows that either BzATP (black squares) or ATP (gray squares) can induce SMG fluid secretion; however at the submaximal concentration tested,

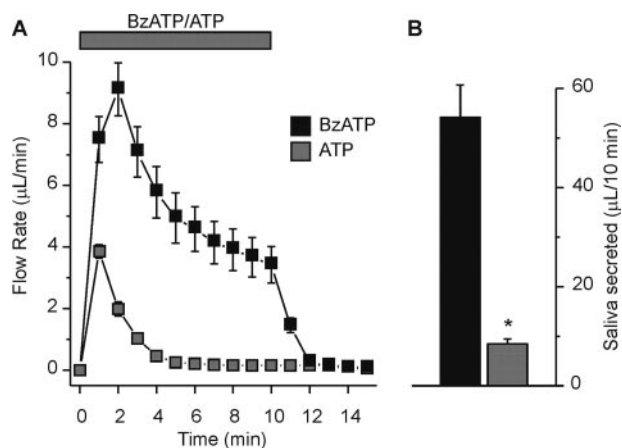


**FIGURE 3. Enhanced SMG fluid secretion evoked by the  $\text{P2X}_7$ -selective agonist BzATP.** Agonists were applied to the *ex vivo*, perfused SMG for 10 min as indicated by the gray bar. **A**, flow rate from the *ex vivo*, perfused SMG following stimulation with  $0.25 \text{ mM}$  of either BzATP (black squares) or ATP (gray squares). **B**, summary of the total volume of fluid secreted over a 10-min stimulation period. Data were from an equal number of male and female animals (BzATP and ATP,  $n = 12$  and  $n = 8$  glands, respectively; \*,  $p < 0.001$ ). Black Swiss/129 SvJ mice were used for these experiments.

BzATP was much more effective (>6-fold at  $0.25 \text{ mM}$ ). In addition, the ATP response was not typically sustained at this concentration of agonist; *i.e.* the majority of the glands quit secreting after 5 min of stimulation, whereas secretion was sustained with BzATP (Fig. 3A). Fig. 3B shows that the volume of BzATP-evoked SMG fluid secretion was significantly greater than the volume secreted by an equal concentration of ATP ( $0.25 \text{ mM}$  BzATP;  $54.2 \pm 6.6 \mu\text{L}/10 \text{ min}$  versus  $0.25 \text{ mM}$  ATP;  $8.4 \pm 1.0 \mu\text{L}/10 \text{ min}$ ,  $p < 0.001$ ). Higher concentrations of ATP ( $1 \text{ mM}$ ) resembled the results using a lower BzATP concentration (compare Figs. 1A and 3A), suggesting that ATP-stimulated fluid secretion is mediated by the BzATP-sensitive,  $\text{P2X}_7$  purinergic receptor.

**Loss of the BzATP-induced Cation Current in  $\text{P2X}_7$  Receptor-null Mice**—Collectively, the observations that extracellular  $\text{Ca}^{2+}$  was required for fluid secretion (Fig. 2) and BzATP was the most potent agonist (Fig. 3) implied that  $\text{P2X}_7$  receptor activation was primarily responsible for the sustained ATP-mediated fluid secretion. One caveat of pharmacological inhibitors of purinergic P2 receptors is that they are not selective and may affect other channels and transporters required for fluid secretion (16). Thus, to confirm the critical role of  $\text{P2X}_7$  receptor activation in stimulating fluid secretion we utilized  $\text{P2X}$  gene-disrupted mice.

Western blot analysis using a  $\text{P2X}_7$  receptor-specific antibody demonstrated that plasma membrane proteins isolated from  $\text{P2X}_7^{-/-}$  mice lacked  $\text{P2X}_7$  receptor protein expression in SMG, parotid (PG), and sublingual (SLG) salivary glands (Fig. 4A, see arrow). As an additional positive control and to confirm protein size, the cell lysate from HEK-293 cells transiently overexpressing the  $\text{P2X}_7$  receptor was included in the analysis (Fig. 4A, lane 7). Fig. 4 also shows that the large BzATP-induced inward cation current present in SMG acinar cells from wild-type mice was absent in  $\text{P2X}_7^{-/-}$  SMG acinar cells (Fig. 4, B and C;  $\text{P2X}_7^{+/+}$ ;  $-349.8 \pm 88.5 \text{ pA}$  versus  $\text{P2X}_7^{-/-}$ ;  $-2.2 \pm 2.3 \text{ pA}$ ,  $p < 0.01$ ). Together, these data demonstrated that disruption of

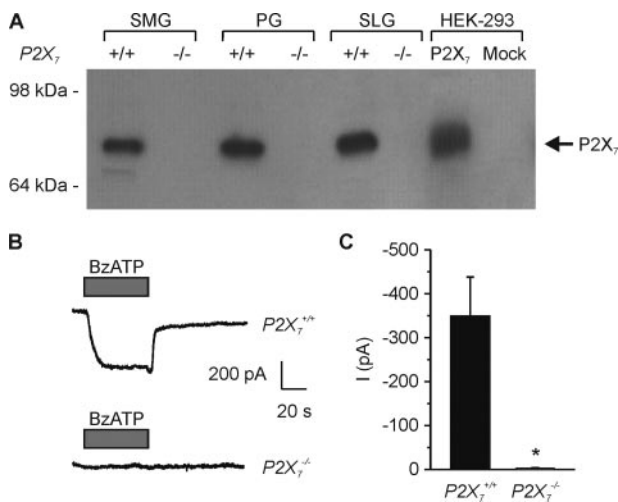


**FIGURE 4. SMG isolated from  $P2X_7^{-/-}$  mice lacked  $P2X_7$  protein expression and BzATP-activated cation currents.** *A*, immunoblot of biotinylated membrane protein samples probed with a  $P2X_7$  receptor specific antibody.  $P2X_7$  receptor protein expression was absent in all three salivary gland tissues from  $P2X_7^{-/-}$  animals. HEK-293 cells were transiently transfected as previously described (9), and cell lysates from mock-transfected and  $P2X_7$  receptor-expressing cells were included as controls and to confirm  $P2X_7$  protein size (see arrow). *B*, representative traces of BzATP (0.25 mM) induced inward cation currents from SMG acinar cells isolated from  $P2X_7^{+/+}$  (upper panel) and  $P2X_7^{-/-}$  (lower panel) mice. *C*, data summary shows the average inward currents following BzATP stimulation ( $P2X_7^{+/+}$  versus  $P2X_7^{-/-}$ ,  $n = 9$  and  $n = 8$ , respectively; \*,  $p = 0.003$ ). Data were from experiments from at least three animals.  $P2X_7^{+/+}$  or  $P2X_7^{-/-}$  C57Bl/6J mice were used for these experiments.

the  $P2X_7$  gene results in loss of both  $P2X_7$  receptor protein expression and nucleotide-gated channel activity.

**$P2X_7$  Receptor Disruption Has No Effect on CCh-evoked Fluid Secretion and  $[Ca^{2+}]_i$  Signals**—We next determined if disruption of  $P2X_7$  receptors in the SMG had nonspecific effects on the fluid secretion machinery. To evaluate this we utilized the muscarinic receptor agonist CCh, the response to which should be unaffected in  $P2X_7$ -null mice. Fig. 5A shows that the *ex vivo* salivary flow rates in  $P2X_7^{+/+}$  (black squares) and  $P2X_7^{-/-}$  (gray squares) SMG were effectively identical in response to CCh stimulation. There were only subtle differences in the total volumes secreted in 10 min ( $P2X_7^{+/+}$ ;  $135 \pm 5 \mu\text{L}/10 \text{ min}$  versus  $P2X_7^{-/-}$ ;  $144 \pm 6 \mu\text{L}/10 \text{ min}$ ,  $p = 0.25$ ), saliva ion compositions (Table 1), or osmolalities ( $P2X_7^{+/+}$ ;  $183.9 \pm 4.5 \text{ mOsm}$  versus  $P2X_7^{-/-}$ ;  $186.0 \pm 3.3 \text{ mOsm}$ ,  $p = 0.74$ ). The lack of effect of  $P2X_7$  receptor ablation on the CCh-stimulated response demonstrated that ion channels and transporters responsible for fluid secretion in SMG are not affected when the  $P2X_7$  gene is disrupted.

Given that salivary gland fluid secretion is dependent on an elevation of  $[Ca^{2+}]_i$ , we expected that disruption of  $P2X_7$  receptors would also have no effect on CCh-evoked  $Ca^{2+}$  signals in SMG acinar cells. To confirm this, SMG acini were isolated and loaded with the  $Ca^{2+}$ -sensitive dye Fura-2. In support of the fluid secretion data, Fig. 5B shows that the CCh-induced  $Ca^{2+}$  signals in  $P2X_7^{+/+}$  (black trace) and  $P2X_7^{-/-}$  (gray trace) isolated SMG acinar cells were essentially identical. Analysis of the data showed that the average peak value over baseline of the CCh-induced  $Ca^{2+}$  signal for  $P2X_7^{+/+}$  cells was not significantly different from that for  $P2X_7^{-/-}$  cells (Fig. 5B,  $P2X_7^{+/+}$ ;  $0.30 \pm 0.02$  ratio units versus  $P2X_7^{-/-}$ ;  $0.33 \pm 0.03$  ratio units,

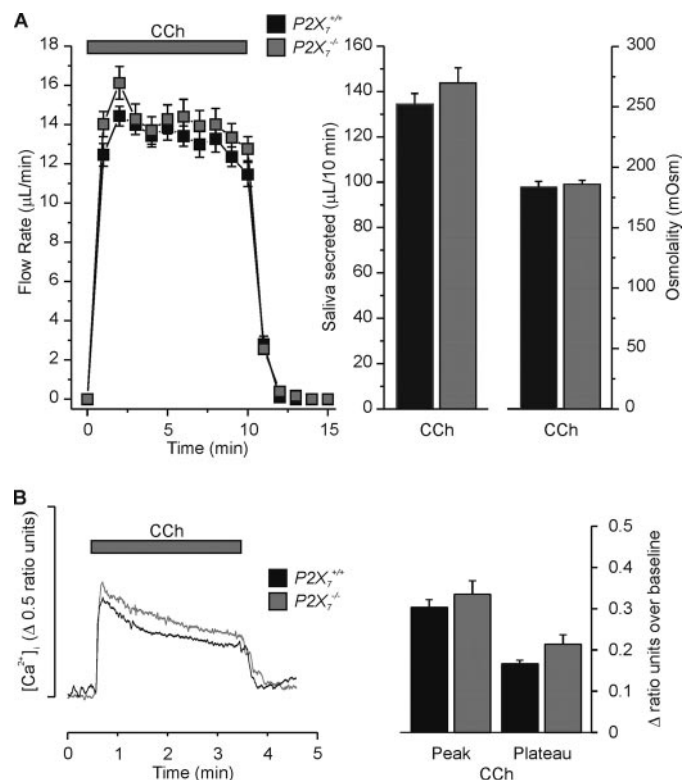


**FIGURE 5. CCh evoked SMG fluid secretion and  $[Ca^{2+}]_i$  signals in  $P2X_7^{+/+}$  and  $P2X_7^{-/-}$  mice.** *A*, *ex vivo* SMG flow rate (left panel), total saliva volume over a 10-min stimulation period (middle panel), and the osmolality (right panel) in response to CCh (0.3  $\mu\text{M}$ ). There was no significant difference between  $P2X_7^{+/+}$  and  $P2X_7^{-/-}$  animals for the total volume secreted ( $P2X_7^{+/+}$  versus  $P2X_7^{-/-}$ ,  $n = 20$  glands and  $n = 17$  glands, respectively,  $p = 0.23$ ) or osmolality ( $P2X_7^{+/+}$  versus  $P2X_7^{-/-}$ ,  $n = 12$  and  $n = 8$  respectively,  $p = 0.74$ ). *B*, Fura-2 loaded SMG acinar cells were stimulated with CCh (0.3  $\mu\text{M}$ ) for 3 min. The representative  $[Ca^{2+}]_i$  response is shown as a change in ratio units (left panel). The data summary (right panel) shows that there was no significant difference in either the average peak value over baseline [ $P2X_7^{+/+}$ ;  $0.30 \pm 0.02$  ratio units versus  $P2X_7^{-/-}$ ;  $0.33 \pm 0.03$  ratio units,  $n = 9$  (33 cells) and  $n = 9$  (34 cells), respectively,  $p = 0.41$ ] or average plateau value over baseline (taken at 1.5 min into the 3-min stimulation) [ $P2X_7^{+/+}$ ;  $0.17 \pm 0.01$  ratio units versus  $P2X_7^{-/-}$ ;  $0.21 \pm 0.02$  ratio units,  $n = 9$  (33 cells) and  $n = 9$  (34 cells), respectively,  $p = 0.07$ ].  $P2X_7^{+/+}$  and  $P2X_7^{-/-}$  C57Bl/6J mice were used for these experiments.

**TABLE 1**

**Carbachol and ATP stimulated fluid secretion and ion composition in the *ex vivo* SMG of wild type and  $P2X_7^{-/-}$  mice**

ANOVA analyses, followed by a Bonferroni test, were performed for multiple comparisons (see "Experimental Procedures"). The numbers in parentheses equal the number of glands tested for each condition.

	P2X <sub>7</sub> <sup>+/+</sup>		P2X <sub>7</sub> <sup>-/-</sup>	
	CCh	CCh + ATP	CCh	CCh + ATP
Na	37.4 ± 2.6 (20)	44.1 ± 3.3 (21)	39.9 ± 4.6 (17)	47.9 ± 5.8 (10)
K	50.4 ± 3.3 (20)	59.6 ± 2.2 <sup>a</sup> (21)	47.7 ± 2.8 <sup>b</sup> (17)	53.8 ± 3.9 (10)
Cl	89.2 ± 4.6 (20)	85.2 ± 1.7 (21)	82.9 ± 4.3 <sup>a</sup> (17)	100.9 ± 3.3 <sup>b</sup> (10)
pH	7.85 ± 0.07 (8)	7.99 ± 0.09 <sup>a</sup> (8)	7.71 ± 0.03 <sup>b</sup> (9)	7.71 ± 0.06 <sup>b</sup> (10)
μL	135 ± 5 <sup>a</sup> (20)	90 ± 7 <sup>b</sup> (21)	144 ± 6 <sup>a</sup> (17)	130 ± 6 <sup>a</sup> (10)

<sup>a</sup> Values are different from those labeled *b* by at least  $p < 0.03$ .

$p = 0.41$ ). In addition, the average plateau value over baseline (taken at 1.5 min into the 3-min stimulation) of the CCh-induced  $Ca^{2+}$  signal for  $P2X_7^{+/+}$  cells was also similar to that for  $P2X_7^{-/-}$  cells ( $P2X_7^{+/+}$ ;  $0.17 \pm 0.01$  ratio units versus  $P2X_7^{-/-}$ ;  $0.21 \pm 0.02$  ratio units,  $p = 0.07$ ). Thus, disruption of  $P2X_7$  receptors had no significant effect on either CCh-mediated fluid secretion or  $Ca^{2+}$  signaling.

## ATP-stimulated Fluid Secretion

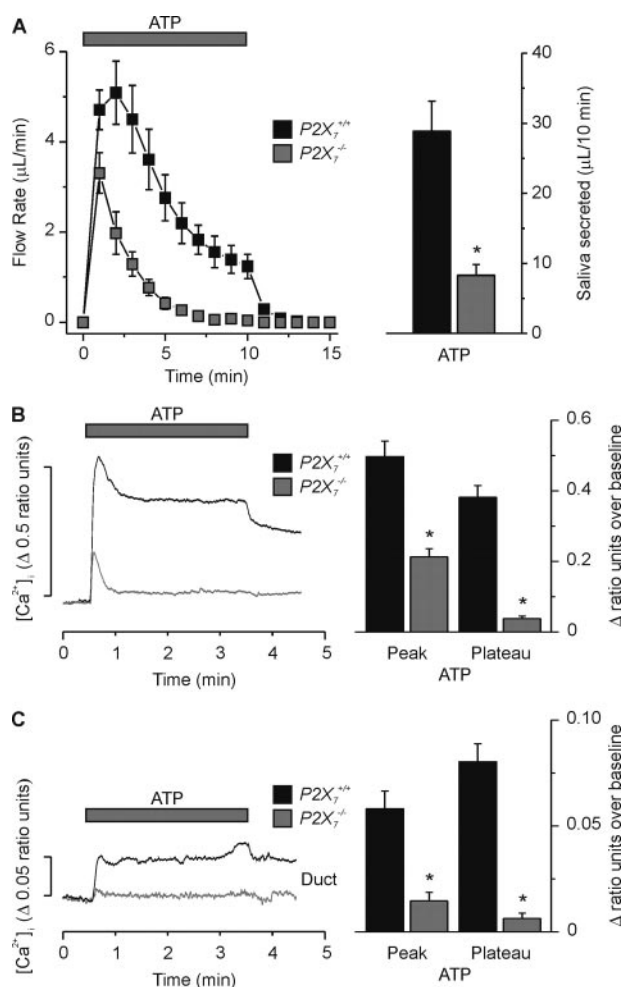


**FIGURE 6. Purinergic receptor agonist-evoked SMG fluid secretion and  $[Ca^{2+}]_i$  signals were decreased in  $P2X_7^{-/-}$  animals.** *A*, *ex vivo* SMG flow rate (left panel) in response to ATP (1 mM). There was a significant decrease in the total volume of SMG fluid secretion (right panel) following ATP stimulation in the  $P2X_7^{-/-}$  animal ( $P2X_7^{+/+}$  versus  $P2X_7^{-/-}$ ,  $n = 12$  glands and  $n = 15$  glands, respectively, \*,  $p < 0.05$ ). *B*, Fura-2 loaded isolated SMG acinar cells were stimulated with ATP (1 mM) for 3 min. The representative  $[Ca^{2+}]_i$  response is shown as a change in ratio units (left panel). There was a significant decrease in both the ATP-evoked average  $Ca^{2+}$  peak [ $P2X_7^{+/+}$ ;  $0.50 \pm 0.04$  ratio units versus  $P2X_7^{-/-}$ ;  $0.21 \pm 0.02$  ratio units,  $n = 8$  (25 cells) and  $n = 9$  (29 cells), respectively, \*,  $p < 0.001$ ] and plateau [ $P2X_7^{+/+}$ ;  $0.38 \pm 0.03$  ratio units versus  $P2X_7^{-/-}$ ;  $0.04 \pm 0.01$  ratio units,  $n = 8$  (25 cells) and  $n = 9$  (29 cells), respectively, \*,  $p < 0.001$ ] in  $P2X_7^{-/-}$  SMG acinar cells. *C*, similar to panel *B*, only Fura-2 loaded SMG granular duct cells. There was a significant decrease in both the ATP-evoked average  $Ca^{2+}$  peak [ $P2X_7^{+/+}$ ;  $0.058 \pm 0.008$  ratio units versus  $P2X_7^{-/-}$ ;  $0.015 \pm 0.004$  ratio units,  $n = 13$  (25 cells) and  $n = 14$  (19 cells), respectively, \*,  $p < 0.001$ ] and plateau [ $P2X_7^{+/+}$ ;  $0.080 \pm 0.008$  ratio units versus  $P2X_7^{-/-}$ ;  $0.006 \pm 0.002$  ratio units,  $n = 13$  (25 cells) and  $n = 14$  (19 cells), respectively, \*,  $p < 0.001$ ] in  $P2X_7^{-/-}$  SMG granular duct cells.  $P2X_7^{+/+}$  or  $P2X_7^{-/-}$  C57Bl/6J mice were used for these experiments.

**Disruption of  $P2X_7$  Receptors Decreases ATP-evoked Fluid Secretion and  $[Ca^{2+}]_i$  Signals**—We next determined if loss of  $P2X_7$  receptor expression had an effect on purinergic receptor agonist-evoked fluid secretion. Fig. 6 shows that the secretion response to the purinergic receptor agonist ATP was markedly reduced in the  $P2X_7^{-/-}$  SMG (gray squares). The total volume of saliva collected over a 10-min period from the  $P2X_7^{-/-}$  SMG was reduced 71% when stimulated with 1 mM ATP (Fig. 6A,  $P2X_7^{+/+}$ ;  $28.9 \pm 4.3$  μl/10 min versus  $P2X_7^{-/-}$ ;  $8.4 \pm 1.5$  μl/10 min,  $p < 0.001$ ). A similar result was obtained when stimulating with the  $P2X_7$ -selective

purinergic receptor agonist BzATP. Fluid secretion evoked by 0.25 mM BzATP decreased by 75% in  $P2X_7^{-/-}$  glands ( $P2X_7^{+/+}$ ;  $50.8 \pm 3.5$  μl/10 min versus  $P2X_7^{-/-}$ ;  $12.6 \pm 1.1$  μl/10 min,  $p < 0.001$ ). Because of the low volume of saliva secreted by either ATP or BzATP in  $P2X_7^{-/-}$  animals, further analyses were not performed.

The most likely mechanism for the dramatic reduction in purinergic receptor agonist-evoked fluid secretion in  $P2X_7^{-/-}$  SMG is impaired  $P2X_7$  receptor-mediated  $Ca^{2+}$  signaling. Consistent with this hypothesis, stimulation of Fura-2 loaded  $P2X_7^{+/+}$  SMG acinar cells with 1 mM ATP for 3 min resulted in an increase in  $[Ca^{2+}]_i$ , which peaked in less than 30 s and then remained at an elevated plateau (Fig. 6B, black trace). Following ATP removal, the  $[Ca^{2+}]_i$  slowly decreased. In contrast, 1 mM ATP stimulation in  $P2X_7^{-/-}$  SMG acinar cells resulted in a transient elevation of  $[Ca^{2+}]_i$ , which returned to near basal levels in less than 30 s (Fig. 6B, gray trace). Analysis of the data showed that the average peak value over baseline of the ATP-induced  $Ca^{2+}$  signal for  $P2X_7^{+/+}$  cells was significantly larger than that for  $P2X_7^{-/-}$  cells (Fig. 6B,  $P2X_7^{+/+}$ ;  $0.50 \pm 0.04$  ratio units versus  $P2X_7^{-/-}$ ;  $0.21 \pm 0.02$  ratio units,  $p < 0.001$ ). In addition, the average plateau value over baseline (taken at 1.5 min into the 3-min stimulation) of the ATP-induced  $Ca^{2+}$  signal for  $P2X_7^{+/+}$  cells was also significantly larger than the average plateau value over baseline for  $P2X_7^{-/-}$  cells (Fig. 6B,  $P2X_7^{+/+}$ ;  $0.38 \pm 0.03$  ratio units versus  $P2X_7^{-/-}$ ;  $0.04 \pm 0.01$  ratio units,  $p < 0.001$ ). In fact, the average plateau value (without baseline subtraction) for  $P2X_7^{-/-}$  cells was not significantly different from the initial value prior to ATP addition (Fig. 6B,  $P2X_7^{-/-}$  plateau;  $0.43 \pm 0.05$  ratio units versus  $P2X_7^{-/-}$  baseline;  $0.39 \pm 0.03$  ratio units,  $p = 0.5$ ).

As previously described (7, 17), we also found that ATP stimulated an increase in  $[Ca^{2+}]_i$  in SMG granular duct cells (Fig. 6C). This  $[Ca^{2+}]_i$  increase peaked in less than 30 s in duct cells and remained elevated (Fig. 6C, black trace). The kinetics of the ATP-induced  $[Ca^{2+}]_i$  increase in granular duct cells were comparable to that observed in acinar cells (*i.e.* there was a rapid  $[Ca^{2+}]_i$  increase after exposure to ATP), although the magnitude of the  $[Ca^{2+}]_i$  peak and plateau values were about an order of magnitude less in duct cells. ATP stimulation in  $P2X_7^{-/-}$  SMG duct cells resulted in a very small, transient elevation of  $[Ca^{2+}]_i$  (Fig. 6C, gray trace). This suggested that  $P2X_7$  receptor activation plays a role in ATP regulation of duct cell  $[Ca^{2+}]_i$  signaling and possibly ion transport function.

**ATP Modulates the Flow Rate of Muscarinic Receptor-stimulated Saliva**—It is unlikely that ATP acts *in vivo* independently of other neurotransmitters like acetylcholine. Therefore, we tested the effects of co-stimulation of the *ex vivo* gland with ATP and CCh on saliva production and ion composition. We found that ATP inhibited CCh-induced secretion by >30% in  $P2X_7^{+/+}$  glands (Fig. 7, A and B, compare black squares and bar to dotted trace and bar). In contrast, ATP failed to inhibit CCh-stimulated secretion in  $P2X_7^{-/-}$  glands (Fig. 7, A and B, gray squares and bar, respectively), suggesting that  $P2X_7$  receptor activation likely mediates the ATP-induced inhibition of the muscarinic receptor response.

The primary, plasma-like saliva generated by acinar cells is modified as it passes through the ducts, which reabsorb NaCl

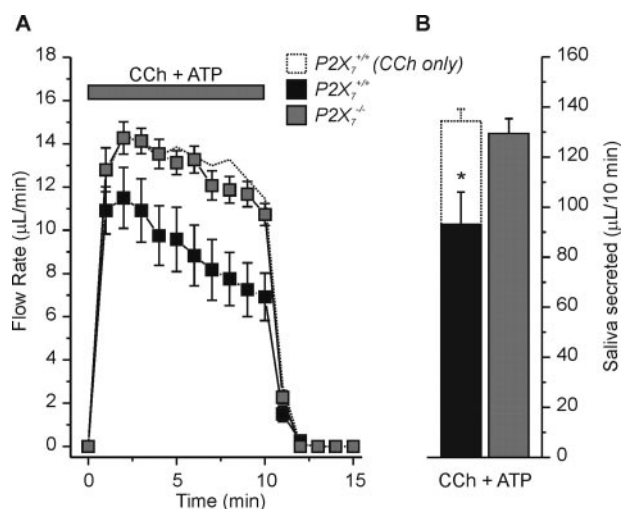


**FIGURE 7. Purinergic receptor agonist induced changes in muscarinic receptor-activated SMG fluid secretion.** A, flow rate from the *ex vivo*, perfused SMG from  $P2X_7^{+/+}$  (black squares) or  $P2X_7^{-/-}$  (gray squares) mice during stimulation with  $0.3 \mu\text{M}$  CCh +  $1 \text{ mM}$  ATP. For comparison the dotted line represents data from  $P2X_7^{+/+}$  mice using  $0.3 \mu\text{M}$  CCh alone from Fig. 5A. B, summary of the total volume of fluid secreted over a 10-min stimulation period. There was no difference in the total volume of SMG fluid secretion between  $P2X_7^{+/+}$  mice stimulated with CCh only (dotted bar) and  $P2X_7^{-/-}$  animals stimulated with CCh + ATP (gray bar) [ $P2X_7^{+/+}$  with CCh only;  $135 \pm 5 \mu\text{L}/10 \text{ min}$ , versus  $P2X_7^{-/-}$  with CCh + ATP;  $130 \pm 6 \mu\text{L}/10 \text{ min}$ ,  $n = 20$  and  $n = 10$  glands, respectively], but both were significantly greater than the total volume of SMG fluid secretion in  $P2X_7^{+/+}$  mice stimulated with CCh + ATP (black bar) [ $P2X_7^{+/+}$  with CCh + ATP;  $90 \pm 7 \mu\text{L}/10 \text{ min}$ ,  $n = 21$ ,  $*$ ,  $p = 0.01$ ].  $P2X_7^{+/+}$  and  $P2X_7^{-/-}$  C57Bl/6J mice were used for these experiments.

and secrete  $\text{KHCO}_3$  (1, 2). ATP stimulated a very modest increase in  $[\text{Ca}^{2+}]_i$  in SMG granular duct cells (Fig. 6C) suggesting that ATP has little influence on duct cell function. Indeed, in  $P2X_7^{+/+}$  mice, ATP did not significantly alter the  $\text{Na}^+$  or  $\text{Cl}^-$  concentration of the saliva induced by CCh stimulation (Table 1); while the pH and the  $\text{K}^+$  concentration of saliva increased slightly. Consistent with these observations, ATP induced only modest changes in the ion composition of saliva from  $P2X_7^{-/-}$  submandibular glands. Taken together, these results suggested that the ATP-stimulated increase in  $[\text{Ca}^{2+}]_i$  in SMG duct cells is unlikely to play a major role in the regulation of ductal function.

## DISCUSSION

Salivary tissues express multiple types of purinergic P2 receptors. Activation of these receptors increases  $[\text{Ca}^{2+}]_i$  suggesting a possible role for P2 receptors in fluid secretion (4, 7, 8, 10, 18, 19), although this has never been directly tested. Here we show that purinergic stimulation results in a sustained, extracellular  $\text{Ca}^{2+}$ -dependent secretion of saliva in an intact mouse submandibular salivary gland preparation. The sensitivity of this response to different purinergic agonists was consistent with  $P2X_7$  receptor activation (BzATP  $\gg$  ATP  $>$  ADP  $\gg$  UTP). Indeed, a  $>70\%$  decrease was observed in BzATP- and ATP-evoked fluid secretions from the SMG in  $P2X_7$ -null animals. These results demonstrate that  $P2X_7$  receptors are essential for ATP-mediated saliva production in the mouse submandibular gland.

Our results highlight the significant contribution purinergic receptors may have on the regulation of salivary gland

fluid secretion. Earlier reports describe a non-adrenergic, non-cholinergic mediated fluid secretion (3, 20–24). In sheep, electrical stimulation of the parotid parasympathetic nerve in the presence of atropine produced a significant increase in the flow rate (25). The authors concluded that the flow rate was produced by vasoactive intestinal peptide (VIP) release (25), however this seems unlikely since VIP receptor activation is linked to an increase in cAMP, not  $[\text{Ca}^{2+}]_i$ . Indeed, Ekstrom *et al.* (26) reported that VIP treatment caused little to no fluid secretion in feline parotid glands. Interestingly, the electrically evoked “atropine-resistant” fluid secretion was  $\sim 30\%$  of the response prior to muscarinic receptor inhibition in the ferret submandibular gland (3). This observation is essentially identical to our results; *i.e.* the maximal volume of ATP-induced fluid secretion was about 30% of that produced by muscarinic receptor stimulation (Fig. 1 versus Fig. 5). Thus, our results are consistent with ATP-mediated fluid secretion playing a physiological role in non-adrenergic, non-cholinergic mediated salivation.

Although both  $P2X_4$  and  $P2X_7$  receptors are expressed in salivary glands, the greater secretion induced by BzATP (Fig. 3) and the severe impairment of secretion in  $P2X_7$ -null mice (Fig. 6) implied that the  $P2X_7$  receptor channel contributes most to salivation. Adding to P2X receptor signaling complexity, functional P2X receptors form heteromeric channels comprised of three P2X subunits (16, 27, 28). Until recently  $P2X_7$  receptors were the only P2X isoform thought not to form a heteromeric channel. However, recent reports have identified  $P2X_4/P2X_7$  heteromeric channels (29, 30). These latter observations suggest that salivary gland cells might contain both  $P2X_4$  and  $P2X_7$  homotrimers, as well as  $P2X_4/P2X_7$  heterotrimers. The functional significance of  $P2X_4/P2X_7$  heterotrimer formation is unclear, but genetic disruption of  $P2X_7$  receptors might also interfere with  $P2X_4$  targeting and/or overall function. Nevertheless, while a  $P2X_4/P2X_7$  heterotrimer is possible, there is no evidence of  $P2X_4/P2X_7$  heterotrimer formation in native tissue. Future studies should be directed to determine the relationship, if any, between  $P2X_4$  and  $P2X_7$  homo- and heterotrimers in salivary gland function.

$P2X_7$  receptors have been previously localized to the apical membrane of mouse parotid acinar and duct cells (8).  $P2X_7$  receptor immunostaining was also noted in mouse SMG duct cells, which suggests that this ligand-gated channel may participate in modification of the electrolyte content (31). Li *et al.* (8) proposed that preassembled  $P2X_7$  receptors in duct cells sense upstream secretion by acinar cells (via ATP release) and respond by augmenting  $\text{HCO}_3^-$  secretion. In agreement with this model, we found that ATP produced a modest increase in the pH of CCh-induced secretions, suggesting an increase in the  $[\text{HCO}_3^-]$ , and this effect disappeared in  $P2X_7$ -null mice (Table 1). Given that ATP is not likely to be released independent of other agonists *in vivo*, ATP might be expected to modulate the response of salivary glands to muscarinic receptor stimulation. Indeed, we also found that the volume of fluid secreted during muscarinic receptor activation was decreased by co-stimulation with ATP and CCh in the *ex vivo* SMG. These results are consistent with the previous observation that ATP inhibits musca-

## ATP-stimulated Fluid Secretion

rinic receptor induced  $\text{Ca}^{2+}$  mobilization in rat parotid and submandibular gland acinar cells (32–34). The inhibition of the CCh-induced response by ATP was absent in  $P2X_7$ -null mice (Fig. 7). Additional studies will be required to confirm the mechanism(s) responsible for these observations. Regardless of the mechanism, our results suggest that ATP can stimulate secretion on its own, and when co-released with a muscarinic agonist, ATP likely modulates the muscarinic receptor-stimulated response of salivary glands. Moreover, the *in vivo* physiologically relevant source of ATP release is unknown. It is well known that ATP is co-released from nerve terminals with acetylcholine and other neurotransmitters (35). Alternatively, ATP is also released from the secretory granules of exocrine acinar cells in response to agonists that stimulate granule fusion (36). The release of ATP from these two distinct sites is likely to have very different functional consequences.

In summary, our results demonstrate that ATP regulates fluid secretion in the mouse submandibular gland. This mechanism is extracellular  $\text{Ca}^{2+}$ -dependent, sensitive to BzATP, and insensitive to UTP, suggesting activation of a P2X receptor family member. Indeed, ablation of the  $P2X_7$  gene resulted in a dramatic reduction in the amount of fluid secreted during ATP exposure. These new findings contribute to our understanding of the role of purinergic P2 receptors in salivary glands and provide insight into future studies. ATP-mediated fluid secretion is likely an important mechanism for “tuning” the resultant fluid secretion under different physiological conditions.

*Acknowledgments*—We thank Laurie Koek, Jennifer Scantlin, Yasna Jaramillo, and Mark Wagner for excellent technical assistance.

### REFERENCES

1. Cook, D. I., Van Lennep, E. W., Roberts, M. L., and Young, J. A. (1994) *Secretion by the Major Salivary Glands*, 3rd Ed., Raven Press, New York
2. Melvin, J. E., Yule, D., Shuttleworth, T., and Begenisich, T. (2005) *Annu. Rev. Physiol.* **67**, 445–469
3. Ekstrom, J., Mansson, B., Olgart, L., and Tobin, G. (1988) *Quart. J. Exp. Physiol.* **73**, 163–173
4. Soltoff, S. P., McMillian, M. K., Cragoe, E. J., Jr., Cantley, L. C., and Talamo, B. R. (1990) *J. Gen. Physiol.* **95**, 319–346
5. Merritt, J. E., and Rink, T. J. (1987) *J. Biol. Chem.* **262**, 14912–14916
6. Burnstock, G. (2007) *Physiol. Rev.* **87**, 659–797
7. Lee, M. G., Zeng, W., and Muallem, S. (1997) *J. Biol. Chem.* **272**, 32951–32955
8. Li, Q., Luo, X., Zeng, W., and Muallem, S. (2003) *J. Biol. Chem.* **278**, 47554–47561
9. Brown, D. A., Bruce, J. I., Straub, S. V., and Yule, D. I. (2004) *J. Biol. Chem.* **279**, 39485–39494
10. Turner, J. T., Landon, L. A., Gibbons, S. J., and Talamo, B. R. (1999) *Crit. Rev. Oral. Biol. Med.* **10**, 210–224
11. Novak, I. (2003) *News Physiol. Sci.* **18**, 12–17
12. Nakamoto, T., Romanenko, V. G., Takahashi, A., Begenisich, T., and Melvin, J. E. (2008) *Am. J. Physiol. Cell Physiol.* **294**, C810–C819
13. Romanenko, V. G., Nakamoto, T., Srivastava, A., Begenisich, T., and Melvin, J. E. (2007) *J. Physiol.* **581**, 801–817
14. Romanenko, V., Nakamoto, T., Srivastava, A., Melvin, J. E., and Begenisich, T. (2006) *J. Biol. Chem.* **281**, 27964–27972
15. Gonzalez-Begne, M., Nakamoto, T., Nguyen, H. V., Stewart, A. K., Alper, S. L., and Melvin, J. E. (2007) *J. Biol. Chem.* **282**, 35125–35132
16. North, R. A. (2002) *Physiol. Rev.* **82**, 1013–1067
17. Pochet, S., Garcia-Marcos, M., Seil, M., Otto, A., Marino, A., and Dehaye, J. P. (2007) *Cell Signal.* **19**, 2155–2164
18. Gallacher, D. V. (1982) *Nature* **296**, 83–86
19. Soltoff, S. P., McMillian, M. K., Lechleiter, J. D., Cantley, L. C., and Talamo, B. R. (1990) *Ann. N. Y. Acad. Sci.* **603**, 76–90; discussion 91–72
20. Asztely, A., Tobin, G., and Ekstrom, J. (1994) *Acta Physiol. Scand.* **151**, 373–376
21. Ekstrom, J. (1998) *Exp. Physiol.* **83**, 697–700
22. Ekstrom, J. (2001) *Exp. Physiol.* **86**, 475–480
23. Ekstrom, J., Asztely, A., and Tobin, G. (1998) *Eur. J. Morphol.* **36**, (suppl.), 208–212
24. Ekstrom, J., Helander, H. F., and Tobin, G. (1993) *J. Physiol.* **472**, 233–244
25. Reid, A. M., and Titchen, D. A. (1988) *Q. J. Exp. Physiol.* **73**, 413–424
26. Ekstrom, J., Asztely, A., Helander, H. F., and Tobin, G. (1994) *Acta Physiol. Scand.* **150**, 83–88
27. Nicke, A., Baumert, H. G., Rettinger, J., Eichele, A., Lambrecht, G., Mutschler, E., and Schmalzing, G. (1998) *EMBO J.* **17**, 3016–3028
28. Torres, G. E., Egan, T. M., and Voigt, M. M. (1999) *J. Biol. Chem.* **274**, 6653–6659
29. Dubyak, G. R. (2007) *Mol. Pharmacol.* **72**, 1402–1405
30. Guo, C., Masin, M., Qureshi, O. S., and Murrell-Lagnado, R. D. (2007) *Mol. Pharmacol.* **72**, 1447–1456
31. Sim, J. A., Young, M. T., Sung, H. Y., North, R. A., and Surprenant, A. (2004) *J. Neurosci.* **24**, 6307–6314
32. Fukushi, Y. (1999) *Eur. J. Pharmacol.* **364**, 55–64
33. Jorgensen, T. D., Gromada, J., Tritsarlis, K., Nauntofte, B., and Dissing, S. (1995) *Biochem. J.* **312**, 457–464
34. Metioui, M., Amsallem, H., Alzola, E., Chaib, N., Elyamani, A., Moran, A., Marino, A., and Dehaye, J. P. (1996) *J. Cell Physiol.* **168**, 462–475
35. Richardson, P. J., and Brown, S. J. (1987) *J. Neurochem.* **48**, 622–630
36. Sorensen, C. E., and Novak, I. (2001) *J. Biol. Chem.* **276**, 32925–32932